



# Expression of the serotonin receptor 2B in uveal melanoma and effects of an antagonist on cell lines

Cindy Weidmann<sup>1,2,3</sup> · Julie Bérubé<sup>1,2,3</sup> · Léo Piquet<sup>1,2,3,5</sup> · Arnaud de la Fouchardière<sup>4</sup> · Solange Landreville<sup>1,2,3,5</sup> 

Received: 17 October 2017 / Accepted: 23 April 2018  
© Springer Science+Business Media B.V., part of Springer Nature 2018

## Abstract

Uveal melanoma (UM) is the most common primary tumor in the adult, and disseminates to the liver in half of patients. A 15-gene expression profile prognostic assay allows to determine the likelihood of metastasis in patients using their ocular tumor DNA, but a cure still remains to be discovered. The serotonin receptor 2B represents the discriminant gene of this molecular signature with the greatest impact on the prognosis of UM. However, its contribution to the metastatic potential of UM remains unexplored. The purpose of this study was to investigate the effects of a selective serotonin receptor 2B antagonist on cellular and molecular behaviours of UM cells. UM cell lines expressing high level of serotonin receptor 2B proteins were selected by Western blotting. The selective serotonin receptor 2B antagonist PRX-08066 was evaluated for its impact on UM cells using viability assays, phosphorylated histone H3 immunostainings, clonogenic assays, migration assays, invasion assays and membrane-based protein kinase phosphorylation antibody arrays. The pharmacological inhibition of the serotonin receptor 2B reduced the viability of UM cells and the population in mitosis, and impaired their clonogenicity and potential of migration. It also decreased the phosphorylation of kinases from signaling pathways classically activated by the serotonin receptor 2B, as well as kinases  $\beta$ -catenin, Proline-rich tyrosine kinase 2, and Signal transducer and activator of transcription 5. Our findings support a role for the serotonin receptor 2B in the proliferation and migration of UM cells, through activation of many signaling pathways such as WNT, Focal adhesion kinase and Janus kinase/STAT.

**Keywords** Uveal melanoma · Serotonin receptor 2B · Antagonist PRX-08066 · Kinases · Metastasis

## Abbreviations

BAP1 BRCA1 associated protein 1  
ERK1/2 Extracellular signal-regulated kinases 1 and 2  
FAK Focal adhesion kinase

GNAQ G protein subunit alpha q  
GNA11 G protein subunit alpha 11  
GSK3 $\beta$  Glycogen synthase kinase 3 beta  
HCC Hepatocellular carcinoma  
HTR2B Serotonin receptor 2B  
JAK Janus kinase  
PDGFRB Platelet derived growth factor receptor beta  
PH3 Phosphorylated form of histone H3  
PYK2 Proline-rich tyrosine kinase 2  
STAT5 Signal transducer and activator of transcription 5  
SRC SRC proto-oncogene non-receptor tyrosine kinase  
UM Uveal melanoma

**Electronic supplementary material** The online version of this article (<https://doi.org/10.1007/s10585-018-9894-x>) contains supplementary material, which is available to authorized users.

✉ Solange Landreville  
Solange.Landreville@fmed.ulaval.ca

- <sup>1</sup> Axe Médecine régénératrice and Centre Universitaire d'Ophthalmologie (CUO)-Recherche, Centre de recherche du CHU de Québec, Quebec City, QC, Canada
- <sup>2</sup> Centre de recherche sur le cancer de l'Université Laval, Quebec City, QC, Canada
- <sup>3</sup> Centre de recherche en organogénèse expérimentale de l'Université Laval/LOEX, Quebec City, QC, Canada
- <sup>4</sup> Département de biopathologie, Centre Léon Bérard, Lyon, France
- <sup>5</sup> Département d'ophtalmologie, Faculté de médecine, Université Laval, Quebec City, QC, Canada

## Introduction

Uveal melanoma (UM) arises from neural crest-derived melanocytes of the uveal tract and represents the most frequent primary intraocular tumor in adults [1]. Liver metastasis is

a dreaded complication of this cancer despite the efficient treatment of the eye by radiation therapy or enucleation [2, 3]. Patients rarely survive more than 5 years following the initial detection of metastasis, with a death rate of 92% at 2 years [4].

Several clinical, histopathological, and genetic factors are associated with UM poor prognosis, such as large tumor size, ciliary body involvement, epithelioid cell type, monosomy of chromosome 3, and *BAP1* (BRCA1 associated protein 1) mutations [5–8]. In addition, a genetic test that can predict the risk of metastasis in UM patients by analyzing simultaneously the expression of 15 genes in the DNA of their ocular tumor was recently implemented in many ocular oncology centers [9, 10]. This test designates the patient's tumor as Class 1 (low risk) or Class 2 (high risk) of developing metastasis, and the serotonin receptor 2B (HTR2B) is the most discriminant gene of this molecular signature; its overexpression is related to the metastatic disease [10].

In addition to its function as a neurotransmitter, serotonin plays a role in development, and most of its biological actions are mediated by G protein-coupled serotonin receptors [11, 12]. These receptors are divided into seven subfamilies, which share overlapping pharmacological properties, and second messenger coupling pathways [12]. HTR2B is involved in cell proliferation and survival through the activation of phospholipase C beta, SRC and Ras-ERK pathways, all mediated by the G protein subunit alpha q (GNAQ) or alpha 11 (GNA11) [13, 14]. Interestingly, both *GNAQ* and *GNA11* genes are frequently mutated in UMs, and the subsequent inactivation of the catalytic domain locks them in their active state [15–17]. HTR2B contributes to eye and craniofacial morphogenesis by preventing the differentiation of neural crest cells (melanocyte precursors) [11, 18]. Its antagonists interfere with neural crest cell migration and lead to their apoptosis [11]. In addition, HTR2B has been described as an oncogene in hepatocellular carcinoma (HCC), as well as in prostate, small intestine, breast and

pancreas cancers [19–23], but as a tumor suppressor in ovarian cancer [24]. Indeed, treatments with selective HTR2B antagonists decreased the viability of HCC, prostate and pancreas cell lines, and impaired the tumor growth in vivo when administered subcutaneously to mice bearing xenografts [19, 22, 23].

The purpose of this study was to investigate the effects of a selective HTR2B antagonist on cellular and molecular behaviors of UM cells. To achieve this, the viability, proliferation, migration, invasion and phosphorylation of various kinases were analyzed after treatments with the antagonist PRX-08066.

## Materials and methods

### Primary tumor samples and tissue culture

This study followed the tenets of the Declaration of Helsinki and was approved by our institutional human experimentation committee (Centre de recherche du CHU de Québec-Université Laval, Quebec City, QC). Human ocular tumor biopsies were collected post-enucleation (Clinique des tumeurs oculaires du CHU de Québec, Quebec City, QC), and confirmed to be UMs by immunohistochemistry by an ocular pathologist (Service de pathologie du CHU de Québec, Quebec City, QC) [25, 26]. Written informed consent was obtained from the enucleated subjects. Pathological data were assessed as previously described (see Table 1 for clinicopathological characteristics and survival data) [27]. UM cell lines T97, T108, T111, T128, T131 and T143 were derived from primary tumors of non-metastatic or metastatic cases (passages 6–12) [25, 26]. UM cell lines, the colorectal adenocarcinoma HT-29 cell line (ATCC, Manassas, VA) and the 3T3 fibroblast cell line were grown in DMEM Low Glucose medium (Wisent, Quebec City, QC), supplemented with 5% fetal bovine serum (FBS; Hyclone, Logan, UT) and

**Table 1** Summary of clinicopathological features, survival data, and mutation status of uveal melanoma patients

Tumor	Sex/age	Date of enucleation	Cell type	Anterior localization	Tumor size (D > 16 mm)	Follow-up <sup>a</sup> (months)	Last status <sup>b</sup>	BAP1 protein loss	Mutant GNAQ Q209	Mutant GNA11 Q209
108	M/44	04/2004	Spindle	No	No	163	ANM	No	No	NA
111	F/63	06/2005	Epithelioid	Yes	Yes	16	DOM	Yes	No	No
128	M/45	10/2008	Epithelioid	Yes	Yes	5	DOM	NA	NA	NA
130	M/44	11/2008	Epithelioid	No	No	108	ANM	No	No	No
131	M/54	12/2008	Epithelioid	Yes	Yes	32	DOM	Yes	NA	NA
143	M/55	03/2011	Spindle	No	No	80	ANM	No	No	No

NA not available (lack of material or Bouin-fixed)

<sup>a</sup>Follow-up: period from enucleation until patient death or last visit

<sup>b</sup>Last status: *DOM* dead of metastasis, *ANM* alive no metastasis

50 µg/mL gentamicin. Normal uveal melanocytes (NUM) were isolated from the choroid of human eyeballs (Centre Universitaire d'Ophthalmologie (CUO)'s Eye Bank, Quebec City, QC) by successive digestions in trypsin and collagenase, and grown using FNC Coating Mix (AthenaES, Baltimore, MD) and a medium optimized for their selection as previously described [28, 29]. All cell lines were tested routinely for mycoplasma infection by PCR (ATCC). The purity of UM and NUM cultures was confirmed by microscopic inspection, hematoxylin and eosin stain, and positivity for MART-1 using 4 µm-thick cell block sections (clone A103, prediluted; Dako, Mississauga, ON) (Supplementary Fig. 1) [27]. BAP1 loss was assessed by immunohistochemistry on 4 µm-thick tissue sections with a BAP1 antibody (C-4 clone, dilution 1:50; Santa Cruz Biotechnology, Dallas, TX) as previously described (Table 1) [30]. Exon 5 of GNAQ and GNA11 genes was screened for mutations by DNA sequencing (ABI 3731 DNA Analyzer; Plateforme de séquençage et de génotypage des génomes, Québec, QC), following PCR amplification with specific primers using DNA extracted from 10 µm-thick tissue sections (Table 1 and Supplementary Table 1).

### Anchorage-independent colony formation assay

UM cell lines were plated in 1.3% methylcellulose (diluted in IMDM medium; R&D Systems, Minneapolis, MN) on untreated 35 mm tissue culture dishes as previously described (10,000 cells per triplicate) [31]. The trypan blue exclusion test was used to take into account cell death after drug treatments. After 14 days of growth, colonies were counted with the Quantity One software version 4.3.0 (Bio-Rad Laboratories, Mississauga, ON) using the Colony Counting tool, after staining with 0.1 mg/mL MTT (Sigma-Aldrich, St. Louis, MO).

### Western blotting

UM cell lines grown to 90% confluency in 100 mm tissue culture dishes were harvested with the TNG-T lysis buffer (50 mM Tris-HCl pH 7.5, 150 mM NaCl, 1% glycerol, 0.1% Triton X-100), supplemented with protease and phosphatase inhibitor cocktails (Roche Diagnostics, Laval, QC) for total protein extraction. The protein concentration was determined with the BCA protein assay kit (Thermo Scientific, St-Laurent, QC), using dilutions of bovine serum albumin for the standards. Western blots were performed using 20–25 µg of total proteins using 1-D SDS-PAGE Stain-Free gels (Bio-Rad Laboratories) and PVDF membranes (GE Healthcare, Mississauga, ON) as an alternative to the most common normalization method using housekeeping proteins. Stain-Free technology enables fluorescent visualization of 1-D SDS-PAGE gels and corresponding blots under UV light using the

Gel Doc Imaging System (Bio-Rad Laboratories). It has a linear dynamic detection range [32, 33]. The relative amount of total proteins in each lane on the blots was calculated with the Quantity One software version 4.3.0 (Bio-Rad Laboratories) using the Volume Tools or the Image Studio Lite software version 5.2.5 (LI-COR Biosciences, Lincoln, NE). The PVDF membranes were then blocked with 5% non-fat dry milk/Tween 0.1% in PBS, and successively incubated with primary antibodies against HTR2B (1:1000; Sigma-Aldrich), β-catenin (1:500; Cell Signaling, Danvers, MA), phosphorylated β-catenin (Ser33/37/Thr41, 1:1000; Cell Signaling), PYK2 (Proline-rich tyrosine kinase 2; 1:500; Cell Signaling), phosphorylated PYK2 (Tyr402, 1:500; Cell Signaling), STAT5 (Signal transducer and activator of transcription 5A; 1:500; Cell Signaling) or phosphorylated STAT5 (Tyr694, 1:500; Cell Signaling), and anti-rabbit or anti-mouse HRP-conjugated secondary antibodies for visualization (1:10,000; Jackson ImmunoResearch Laboratories, West Grove, PA). Immunoreactive complexes were revealed by chemiluminescence using ECL Western blotting substrate (GE Healthcare) and the Fluor S-Max Imaging System (Bio-Rad Laboratories). The relative amount of total HTR2B proteins in each lane on the blots was calculated with the Quantity One software (Bio-Rad Laboratories) using the Volume Tools or the Image Studio Lite software (LI-COR Biosciences). The signal intensities were then normalized with the Stain-Free data.

### Viability assay

UM cell lines were grown in 96-well tissue culture plates (2000 cells/well) in DMEM Low Glucose 5% FBS, and cell viability was measured at 72 h post-treatment with increasing concentrations of PRX-08066 (Selleck Chemicals, Houston, TX) using the MTS assay (tetrazolium salt) according to the manufacturer's instructions (CellTiter 96 Aqueous Assay Reagent; Promega, Madison, WI). The bioreduction of the MTS tetrazolium compound into a colored formazan by metabolically active cells was quantified by recording the absorbance at 490 nm with a microplate reader (Model 550; Bio-Rad Laboratories) [34]. Data are represented as relative percentage of cell viability. The absorbance of untreated cells was considered as 100%.

### Cell proliferation assay

UM cell lines were plated on coverslips (5000 cells/coverslip), fixed 15 min with 4% PFA at 72 h post-treatment with 20 µM PRX-08066 and permeabilized with 0.1% Triton X-100. The blocking of nonspecific sites was performed with 5% goat serum in PBS/0.1% Triton X-100. Mitotic cells were targeted with a primary polyclonal antibody against the phosphorylated form of histone H3 (anti-PH3, dilution

1:1600; Cell signaling), followed by an incubation with a secondary antibody anti-rabbit-Alexa 488 for visualization (1:500; Life Technologies). Nuclei were counterstained with DAPI nuclear stain (Life Technologies). Pictures of six random fields on duplicate coverslips were taken on a epifluorescence microscope at  $\times 20$  magnification (AxioImager 2; Zeiss, Toronto, ON). PH3 positive cells were counted, as well as the total number of nuclei for normalization. Data are represented as percentage of mitotic cells.

### Migration assay

UM cell lines were plated in Culture-Insert 2 Well (35,000 cells/well; Ibidi USA, Madison, WI), with a defined 500  $\mu\text{m}$  cell-free gap. The 3T3 fibroblast cell line was used as positive control of migratory cells. Pictures were taken on a phase contrast microscope (10x magnification) at 72 h post-treatment with 20  $\mu\text{M}$  PRX-08066 (24 h of migration). Image post-processing was carried out using the Image J version 1.46r (<http://rsb.info.nih.gov/ij/>) in order to determine the percentage of wound area closure.

### Invasion assay

UM cell lines grown at 70% of confluence were treated with 20  $\mu\text{M}$  of PRX-08066 for 72 h. The cells were then seeded in CellCarrier-96 Spheroid ULA/C plates (40,000 cells/well in 50  $\mu\text{L}$ ; Perkin-Elmer, Woodbridge, ON) to generate tumoral spheroids in 48 h. A layer of Matrigel Matrix (diluted 1:4; Corning, Corning, NY) was then added onto the spheroids to assess their invasive potential. Phase contrast pictures were taken at Day 0 (after 1 h of incubation) and Day 3 at  $\times 10$  magnification. The diameter of each tumoral spheroid including the invading front was measured with the ImageJ software in order to determine the Day 3/Day 0 ratio of the diameter.

### Human phospho-kinase proteome

The Proteome Profiler Human Phospho-Kinase Array Kit (R&D System, Minneapolis, MN) was used to simultaneously detect the relative levels of phosphorylation of 43 kinase phosphorylation sites (duplicate spots). UM cell lines were treated 72 h with 20  $\mu\text{M}$  PRX-08066 before extracting the total proteins according to the manufacturer's recommendations. 400  $\mu\text{g}$  of total proteins were incubated per membrane, and pixel densities on developed X-ray films were collected and analyzed using the Quick Spots image analysis software (Western Vision, Salt Lake City, UT). The mean density pixels were normalized with the average signal of negative control spots. Data are represented as heatmaps in percentage of relative expression (black, positive control spots = 100%; white, negative control spots = 0%).

### Statistical analysis

Experimental data were presented as column bar graphs (mean  $\pm$  standard error of the mean (SEM)), column mean graphs (mean  $\pm$  SEM), heatmaps, area-proportional Venn diagrams (BioInfoRx Venn Diagram Plotter) or box-and-whisker plots (Prism 7; GraphPad Software, La Jolla, CA). In the latter, the central box is the interquartile range with the median indicated by the horizontal line, and whiskers extend to the lowest and highest data values. Student's *t*-test or Mann–Whitney test were performed to determine statistical significance using Prism 7, and differences were considered to be statistically significant at  $P < 0.05$ . The sample size included data from three independent experiments performed in triplicate with biological replicates.

## Results

### Selection of UM cell lines highly expressing the HTR2B protein

To study the effects of the pharmacological repression of HTR2B in UM, we selected the UM cell lines T111, T128, and T131 derived from the primary tumor of patients with liver metastases. Examination of these cell lines under phase contrast microscopy indicated that they all exhibited an epithelioid morphology (Supplementary Fig. 1), and expressed the melanocyte antigen differentiation marker MART-1. In addition, they formed colonies, demonstrating their anchorage-independent proliferation (Supplementary Fig. 1). We then verified by immunohistochemistry and DNA sequencing the mutation status of *BAP1*, *GNAQ* and *GNA11* in these patients. Tumors 111 and 131 lost the nuclear BAP1 expression, and the tumor 111 was wild-type for exon 5 of *GNAQ* and *GNA11* (Table 1). We were not able to test for mutations the tumor T128 because it was Bouin-fixed, and failed to amplify *GNAQ/GNA11* genes in tumor T131. However, all derived cell lines had no mutation in both genes. High expression of the HTR2B receptor was confirmed by western blotting in all three cell lines, compared to the normal choroid (Fig. 1b). UM cell lines T111, T128 and T131 were thus reliable models to assess in vitro the therapeutic potential of a HTR2B antagonist.

### The HTR2B antagonist PRX-08066 decreased the viability and proliferation of UM cell lines

To determine the cytotoxic effect of the selective HTR2B antagonist PRX-08066, we treated UM cells lines T111, T128, and T131 with increasing concentrations of the drug for 72 h (5–100  $\mu\text{M}$ ; Fig. 2a). By comparison with the untreated control, there was a dose-dependant decreased in

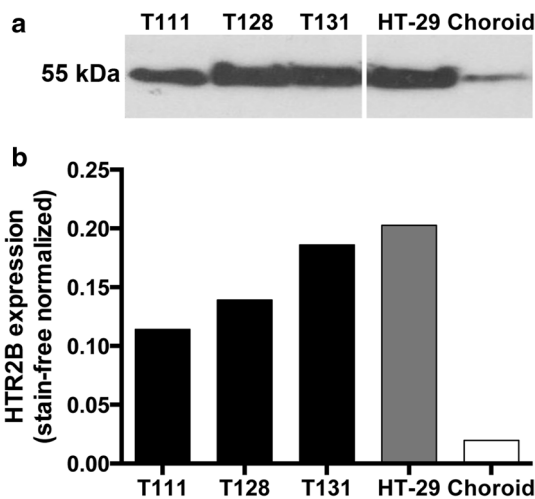


**Fig. 1** Expression of HTR2B in UM cell lines. Western blot conducted on protein extracts from UM cell lines T111, T128 and T131, as well as controls using an antibody against HTR2B (a). The amount of total HTR2B protein per lane was quantified for UM cell lines (black bars), colorectal adenocarcinoma cell line HT-29 (grey bar; positive control) and normal choroid (white bar; normal control), and then normalized with the Stain-Free signal intensities (b)

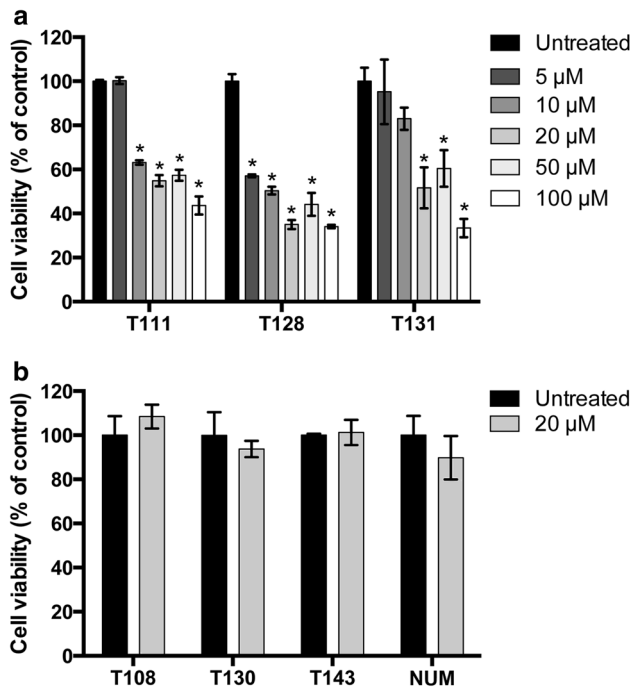


**Fig. 2** The HTR2B antagonist PRX-08066 reduced the viability of UM metastatic cell lines. MTS cell viability assays were performed 72 h post-treatment with PRX-08066. Increasing concentrations of PRX-08066 (5, 10, 20, 50 and 100 μM) were tested on UM metastatic cell lines T111, T128 and T131 (a). The 20 μM concentration was tested on UM non-metastatic cell lines (T108, T130 and T143) and normal uveal melanocytes (NUM; b). Data are represented as relative percentage of viability using a column bar graph (mean ± SEM). The absorbance of untreated cells (black bars) was considered as 100%. Student *t*-test, \**P* < 0.05

the viability of UM metastatic cell lines (Fig. 2a). The sensitivity to PRX-08066 varied slightly between cell lines, and we selected the 20 μM concentration (IC<sub>50</sub>; *P* < 0.05 for all cell lines) to conduct the following experiments. Interestingly, no significant effect was observed in UM non-metastatic cell lines and normal melanocytes at this concentration (Fig. 2b). Because a viable cell is not necessary in a proliferative state, we quantified the population of UM metastatic cells in mitosis 72 h post-treatment with 20 μM PRX-08066 using immunofluorescence analyses with PH3, present only during the M-phase. We observed a decreasing trend in the number of PH3 positive cells in PRX-treated cells (Fig. 3). The reduction was significant for the T111 cell line (−44%, *P* = 0.008).

### The HTR2B antagonist PRX-08066 reduced the self-renewal and potential of migration of UM metastatic cell lines

To determine if the HTR2B receptor promotes the self-renewal of UM metastatic cells, anchorage-independent colony formation assays were performed 72 h post-treatment with 20 μM PRX-08066. As shown in Fig. 4, the number of colonies decreased significantly in treated cells (T111: −87.8%, *P* = 0.0001; T128: −77.9%, *P* = 0.004; T131: −68.9%, *P* = 0.0002) compared to untreated controls. Next, the role of HTR2B in UM cell migration was investigated using culture-inserts 2 Well (Fig. 5a). Interestingly after 24 h, we observed a slower closure of the 500 μm-gap in PRX-treated cells (72 h of treatment), with variability between UM metastatic cell lines (T111: 40.3% of wound area closing, *P* = 0.06; T128: 10.5% of wound area closing,

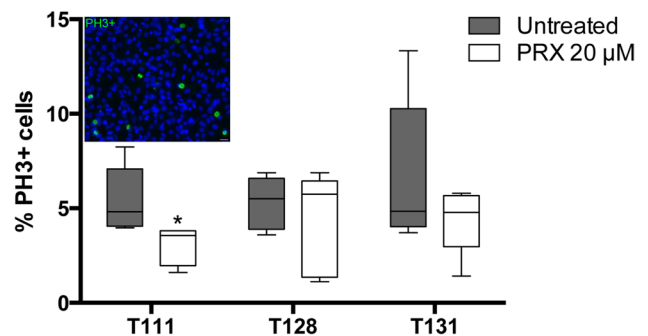


**Fig. 3** The HTR2B antagonist PRX-08066 decreased the proliferation of UM metastatic cell lines. The percentage of mitotic cells was determined in untreated (dark grey boxes) or PRX-treated (20 μM, 72 h; white boxes) UM cell lines T111, T128 and T131 by immunofluorescence analyses using a phospho-histone H3 antibody (PH3). PH3-positive cells (green) were counted, and the total number of DAPI-stained nuclei (blue) was used for normalization. Data are represented as box-and-whisker plots, with median indicated by the horizontal line. Scale bar, 20 μm. Mann–Whitney test, \**P* < 0.05. (Color figure online)

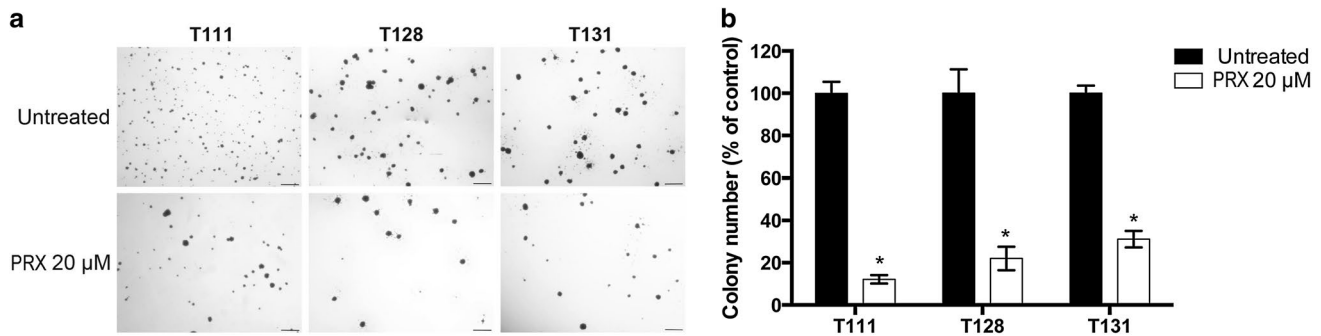


**Fig. 4** The HTR2B antagonist PRX-08066 reduced the self-renewal of UM metastatic cell lines. Phase contrast micrographs of MTT-stained colonies formed by untreated or PRX-treated (20 μM, 72 h) UM metastatic cells T111, T128 and T131 after 14 days in 1.3%

methylcellulose (a). Scale bar, 1 mm. Colony counts are presented as relative number of colonies using a column bar graph (mean ± SEM), where the count of untreated cells (black bars) was considered as 100% (b). Student *t*-test, \**P* < 0.05

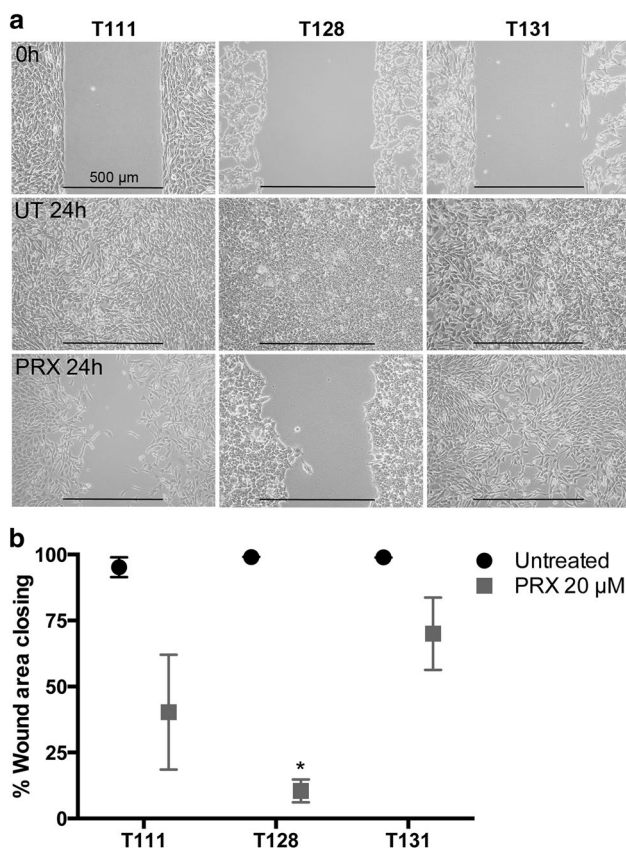


**Fig. 5** The HTR2B antagonist PRX-08066 decreased the migration of UM metastatic cell lines. Phase contrast micrographs of untreated or PRX-treated (20 μM, 72 h) UM metastatic cell lines T111, T128 and T131 (a). Scale bar, 500 μm. The potential of migration is represented as relative percentage using a column mean graph (mean ± SEM), where the wound area closing of untreated cells (black bars) was considered as 100% (b). Student *t*-test, \**P* < 0.05

*P* < 0.0001; T131: 70.0% of wound area closing, *P* = 0.10; Fig. 5b). In comparison, the untreated cells migrated to cover the gap entirely (Fig. 5a). Finally, invasion assays

were performed 72 h post-treatment with 20 μM PRX-08066 using tumoral spheroids embedded in Matrigel (Fig. 6a). We observed a decrease of the invasive potential of the PRX-treated T111 cells after 3 days (−27% of the spheroid diameter, *P* = 0.01; Fig. 6b). The T128 cell line did not grow very well in spheroids and forms rather cell aggregates, so its invasive potential was difficult to assess by this approach. The T131 cell line was the most invasive, but did not respond to the PRX-treatment (−1% of the spheroid diameter, *P* = 0.88; Fig. 6b).

### The HTR2B antagonist PRX-08066 reduced the phosphorylation of various signaling kinases

To identify signaling pathways activated downstream of HTR2B in UM metastatic cell lines, phospho-kinase arrays were performed to analyze the altered expression of kinases 72 h post-treatment with 20 μM PRX-08066 (Fig. 7 and Supplementary Fig. 2). In PRX-treated UM cell lines T111, T128 and T131, 19, 19 and 28 phospho-kinases were significantly downregulated (Fig. 7). Known HTR2B targets such as pERK1/2 (Extracellular signal-regulated kinases 1 and 2), pPDGFRB (Platelet derived growth factor receptor beta) and pSRC (SRC proto-oncogene non-receptor tyrosine kinase) are highlighted with green boxes (Supplementary Fig. 2a–c); only pPDGFRB was significantly decreased in all UM cell lines (Fig. 7a). There were more common targets between UM cell lines T111 and T131 (18 on 19 targets; see Venn diagram in Supplementary Fig. 2d). Moreover, in addition to pPDGFRB, 4 targets were significantly decreased in all UM cell lines: pβ-catenin, pPYK2, pSTAT5A and pSTAT5B (Fig. 7b; red boxes in Supplementary Fig. 2a–c). We validated the expression and activation of β-catenin, PYK2 and STAT5 by Western blotting (Fig. 8). The treatment with PRX reduced the expression of all total proteins in all cell lines. The level of phosphorylation of the β-catenin was decreased only in the T111 cell line after normalization with

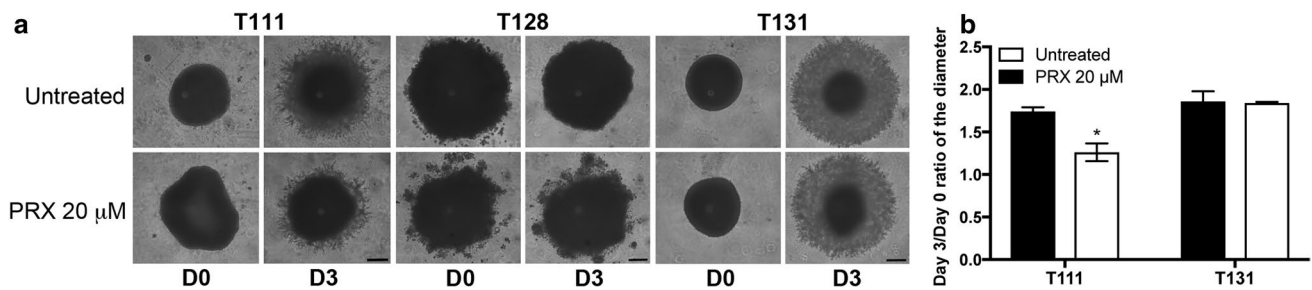


**Fig. 6** The HTR2B antagonist PRX-08066 decreased the invasion of UM metastatic cell lines. Phase contrast micrographs of untreated or PRX-treated (20  $\mu$ M, 72 h) tumoral spheroids of UM metastatic cell lines T111, T128 and T131 (a). Scale bar, 200  $\mu$ m. The potential of

invasion of cell lines T111 and T131 is represented as Day 3 (D3)/Day 0 (D0) ratio of the spheroid diameter using a column mean graph (mean  $\pm$  SEM) (b). Student *t*-test, \**P* < 0.05

the total protein (Fig. 8a). The pPYK2 level was lower in PRX-treated T111 and T128 cell lines (Fig. 8b). The phosphorylated form of STAT5 was decreased in all three UM metastatic cell lines (Fig. 8c). However, Western blotting is less sensitive (ng of proteins) than the proteome array (pg/mL) in terms of detection. The Fig. 7c depicts the other deregulated phospho-kinases for each cell line; several are identified in at least two cell lines (see Venn diagram in Supplementary Fig. 2d). These findings together support that HTR2B positively regulates in UM metastatic cell lines the activity of the JAK (Janus kinase)/STAT, FAK (Focal adhesion kinase) and WNT signaling pathways, which are involved in cell proliferation, migration and self-renewal.

## Discussion

HTR2B has been described as an oncogene in several cancers [19–23]. The HTR2B transcript is overexpressed in metastatic UMs [10], but its functional role is still undetermined in the progression of this cancer. Only a few studies have been conducted to assess the therapeutic potential of HTR2B antagonists in cancer [19, 21–23], but they were tested in clinical trials for the treatment of several diseases such as pulmonary arterial hypertension [35–37], migraine [38, 39], and irritable bowel syndrome [40, 41]. We are the first to investigate the effects of the selective HTR2B antagonist PRX-08066 on the viability, proliferation, migration and expression of signaling kinases in UM metastatic cell lines. The pharmacological repression of HTR2B reduced the population of UM cells in mitosis, impaired their clonogenicity and migration potential, and decreased the phosphorylation of kinases typically activated by HTR2B, as well as new targets such as  $\beta$ -catenin, PYK2 and STAT5.

The passage number dramatically alters the phenotypic and genotypic characteristics of cancer cell lines [42]. For example, long-term subculture affects the molecular signature in UM cells [26]. Moreover, we performed our assays

at low passage number (<P12), and initially confirmed by Western blotting that our UM metastatic cell lines all expressed a high level of HTR2B similar to the positive control colorectal adenocarcinoma HT-29 cell line. Interestingly, the selective HTR2B antagonist PRX-08066 decreased the viability of UM cell lines at micromolar concentrations only for UM metastatic cells, compared to low-grade UM cell lines and normal melanocytes. We did test other selective antagonists of HTR2B such as SB-204741 and RS-127445; the results were similar when using higher concentrations of both drugs (IC<sub>50</sub> = 50–100  $\mu$ M; data not shown). It was shown previously that HTR2B antagonists decreased the viability of cancer cell lines derived from prostate, pancreas and small intestinal neuroendocrine tumors as well as HCC [19, 21–23]. In addition, we observed an interindividual variability in the sensitivity to PRX-08066 treatments in UM metastatic cell lines, particularly for cell proliferation, migration and invasion, reflecting genetic differences between patients or the activation of compensatory signaling mechanisms.

Our analyses of the proliferation rate using PH3 staining showed a decreasing trend in mitotic cells in the PRX-treated group. This anti-proliferative effect was also observed in small intestinal neuroendocrine tumors, where the number of Ki67-positive cells dropped by 33% after treatments with PRX-08066 [21]. In addition, the selective HTR2B antagonist SB-215505 reduced by 20% the percentage of prostate cancer cells in S-phase [19]. Besides, we observed a reduction of phosphorylated  $\beta$ -catenin and STAT5 in our PRX-treated UM cell lines.  $\beta$ -catenin is normally confined to the cell membrane, but is expressed under its phosphorylated form in the cytoplasm and/or nucleus in melanoma cells [43–45]. It was shown previously that the pharmacological inhibition of  $\beta$ -catenin decreased the growth of both uveal and skin melanoma cell lines [45, 46]. Next, STAT proteins are transcription factors activated by cytokines and growth factor receptors, and they are involved in mitogenic and anti-apoptotic signaling [47]. To the best of our knowledge, we are the first to report its constitutive activation in UM. In skin

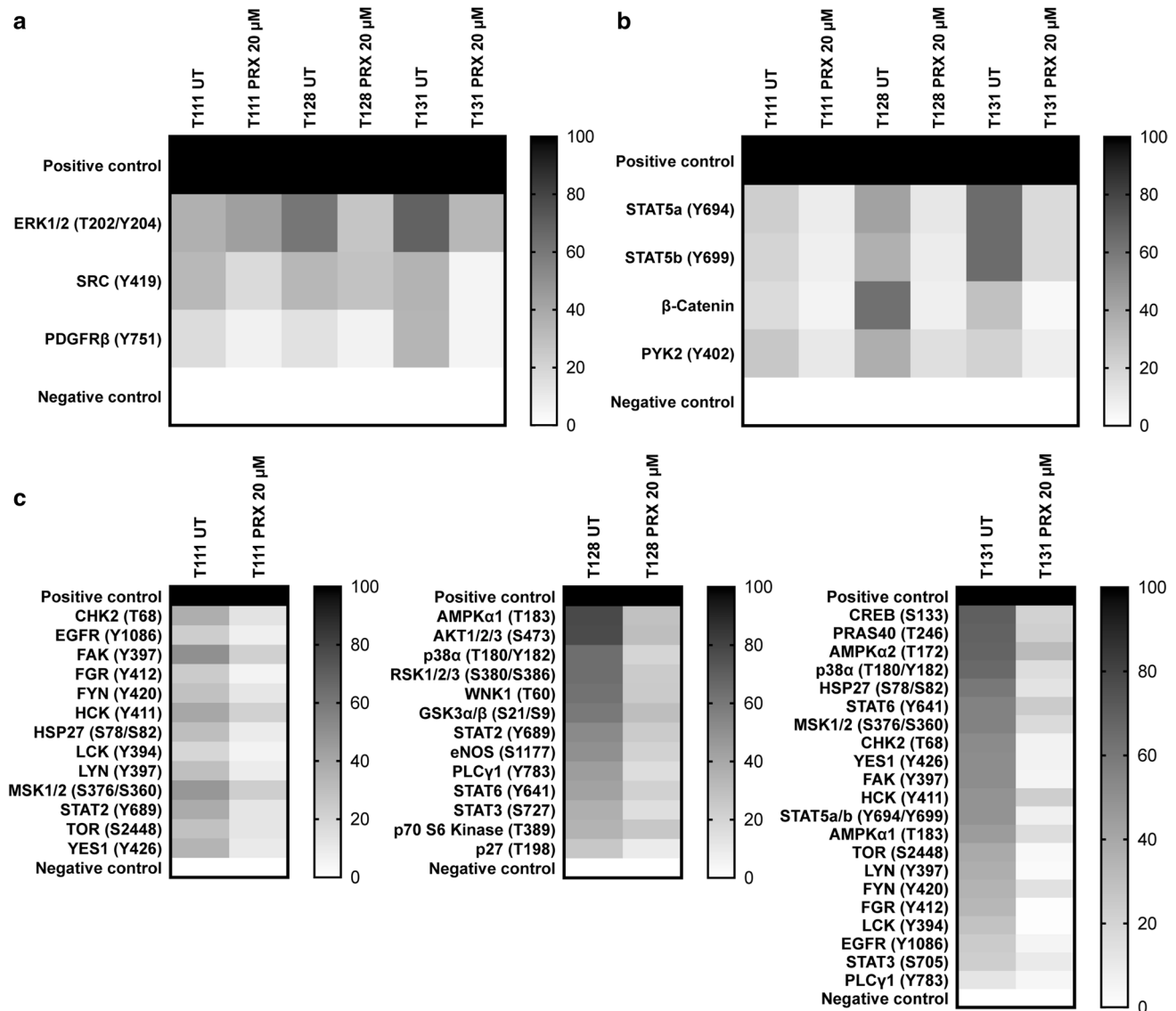


**Fig. 7** The HTR2B antagonist PRX-08066 reduced the phosphorylation of various signaling kinases. Heatmap of the relative expression of known HTR2B targets pERK1/2, pPDGFRB and pSRC in untreated (UT) and PRX-treated (20  $\mu$ M, 72 h) UM cell lines (**a**). Heatmap of the relative expression of p $\beta$ -catenin, pPYK2, pSTAT5A and pSTAT5B that were significantly decreased in all PRX-treated

UM cell lines (**b**). Heatmap of the relative expression of other phospho-kinases reduced post-PRX treatment in each UM cell line (**c**). The expression of each kinase was tested in duplicates. The corresponding quantifications are presented as percentage of relative expression in grayscale, where the positive controls appear in black (100%), and the negative controls in white (0%)

melanoma, pSTAT5 enabled cancer cells to overcome the interferon alpha-mediated anti-proliferative signaling [48]. Its inhibition by RNA interference induced a G1 cell arrest in these cells through the downregulation of cyclin D2 [49], thus supporting its role in cell cycle progression.

Using anchorage-independent colony formation assays, we demonstrated that the antagonist PRX-08066 reduced significantly the number of colonies generated by UM metastatic cell lines, thus supporting that HTR2B plays a role in their clonogenicity. Deregulated phosphorylated kinases identified in our study, such as  $\beta$ -catenin, PYK2 and STAT5,

were all previously linked to cancer stem cell self-renewal [50–53]. Thereby, it was shown in breast cancer cells that the activation of  $\beta$ -catenin and PYK2 increases the formation of mammospheres [50, 51]. Anchorage-independent survival and proliferation of small cell lung cancer cells were as well inhibited when PYK2 was knockeddown [52]. Likewise, the inhibition of STAT5 by RNA interference or with a specific inhibitor reduced the number and volume of hepatospheres in HCC [53].

It is known that HTR2B antagonists interfere with melanocyte precursor migration [11]. We thus hypothesized

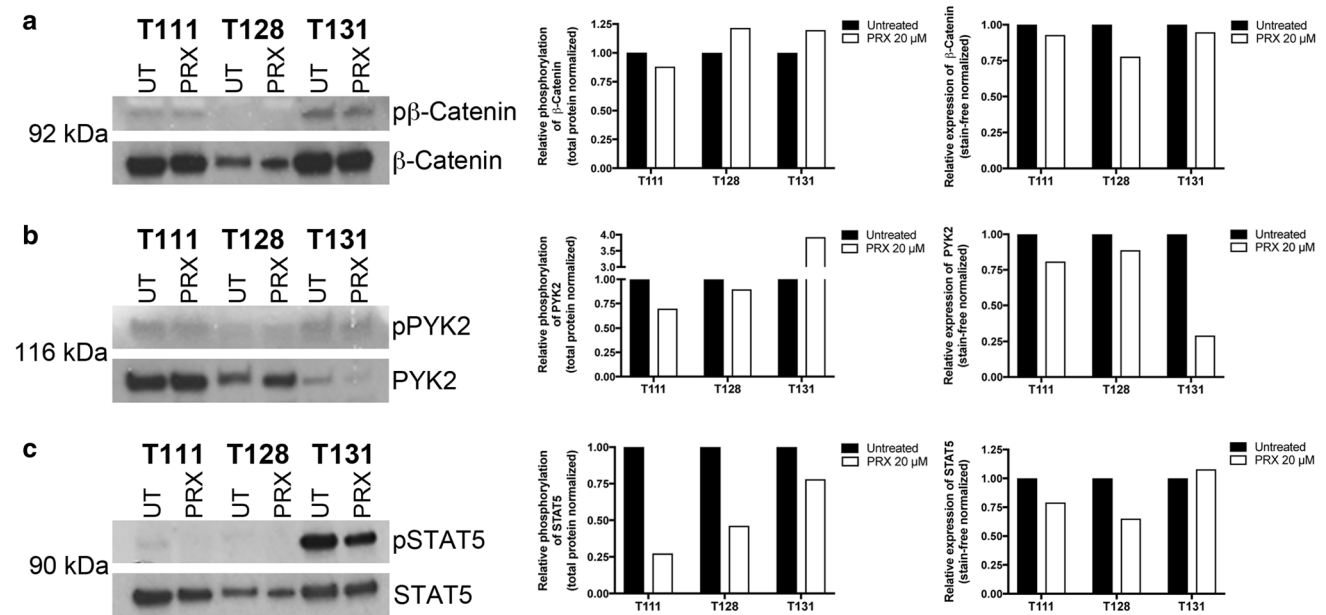


**Fig. 8** Expression and activation of  $\beta$ -catenin, PYK2 and STAT5 proteins in UM cell lines. Western blots conducted on protein extracts from untreated or PRX-treated (20  $\mu$ M, 72 h) UM cell lines T111, T128 and T131 using antibodies against total and phosphorylated  $\beta$ -catenin (a), PYK2 (b) and STAT5 (c). The amount of each protein

per lane was quantified for untreated (black bars) and PRX-treated (white bar) UM cell lines, and then normalized with the Stain-Free signal intensities (total protein) and with the total protein (phosphorylated protein)

that HTR2B can promote metastatic spreading of UM cells. Indeed, our migration assays demonstrated a reduction of the cell motility and invasion in PRX-treated UM cells. The anti-migrative effect of PRX-08066 was previously observed in small intestinal neuroendocrine tumors [21]. Among the deregulated phospho-kinases detected in our proteomes,  $\beta$ -catenin, PYK2 and STAT5 were all previously associated to melanoma progression or enhanced motility/invasiveness. Indeed, cytoplasmic/nuclear p $\beta$ -catenin is significantly correlated to poor prognosis and invasive motility in uveal and skin melanomas [43, 44, 46]. Overexpression of PYK2 is correlated with increased metastasis and cell migration in HCC as well as breast and non-small cell lung cancers [54–56]. This focal adhesion protein upregulates the formation of lamellipodia and actin stress fiber polymerization when phosphorylated [55]. Finally, STAT5 is phosphorylated in 60% of skin melanoma metastases compared to normal melanocytes [49], and the number of cells showing intranuclear localization increased from benign to metastatic lesions [48].

Using phospho-kinase arrays, we discovered that the phosphorylation of kinases such as  $\beta$ -catenin, PYK2, STAT5A and STAT5B was significantly reduced in PRX-treated UM cell lines, in addition to classical targets downstream of HTR2B (ERK1/2, PDGFRB, SRC). It was shown recently that an antagonist of the serotonin receptor HTR7 decreased the phosphorylation of  $\beta$ -catenin in HCC [57],

and that HTR1D promoted colorectal cancer metastasis by activating  $\beta$ -catenin [58], thus suggesting that this pathway can be activated by serotonin. Interestingly, many of the kinases highlighted in our study interact with each other. Indeed, SRC regulates  $\beta$ -catenin and STAT5 in skin melanoma [49, 59, 60], acts with PYK2 to activate the MAPK signaling pathway downstream of Gq-coupled receptors [61], and is indispensable for the phosphorylation of PYK2 in response to cell attachment [62]. In addition, PYK2 inactivates GSK3 $\beta$  (Glycogen synthase kinase 3 beta) by phosphorylation to turn on the WNT/ $\beta$ -catenin signaling pathway [63], mediates cell–cell adhesion by controlling the phosphorylation of  $\beta$ -catenin [64], and promotes epithelial to mesenchymal transition via its association with STAT5B [65]. Furthermore, HTR2B regulates cell-cycle progression through cyclin D1 under the control of SRC in concert with PDGFR [14].

Interestingly, under metabolic stress, HTR2B-positive pancreatic cancer cells acquired a growth advantage by metabolizing more glucose by aerobic glycolysis (Warburg effect) rather than through oxidative phosphorylation [23]. Aiming a particular metabolic pathway may have limited anticancer effects, but interfering with the metabolic plasticity of cancer cells by targeting upstream regulators such as HTR2B can make the cells more sensitive to cytotoxic drugs. In addition, serum serotonin levels have been shown to increase significantly in patients with liver diseases or

HCC [66], and HTR2B is selectively expressed by activated hepatic stellate cells [67], which promote metastatic growth [68]. Selective antagonists of HTR2B may therefore achieve a more durable clinical response in UM patients with liver metastasis, by acting both as anti-proliferative/migrative and anti-fibrotic agents on HTR2B-positive metastatic UM cells and hepatic stellate cells.

**Acknowledgements** The authors would like to thank Dr. Dan Bergeron, Dr. Alain Rousseau and Mrs. Marcelle Giasson for clinical follow-up data, Dr. Daniel O. Black, Dr. Yvonne Molgat and Dr. Mohib W. Morcos for UM tumor surgical samples, as well as the nurses Mrs. Marthe Mercier, Sylvie Marcoux, Suzanne Boulianne, Louise Monroe, and Jocelyne Boivin for the recruitment of patients. They are also grateful to Mrs. Michèle Orain for her technical assistance with archived specimens. S.L. is a Research Scholar of the Fonds de recherche du Québec - Santé (FRQS). C.W. was supported by scholarships from the Faculté de médecine de l'Université Laval, the Fondation du CHU de Québec and the Centre de recherche en organogénèse expérimentale de l'Université Laval/LOEX. L.P. is supported by scholarships from the Fondation d'ophtalmologie, recherche et développement, and the Eye Disease Foundation. This work was supported by grants from the FRQS, the Canadian Foundation for Innovation, the Fondation du CHU de Québec, the Eye Disease Foundation, the Fondation d'ophtalmologie, recherche et développement, and the Fondation de l'Université Laval. The FRQS Vision Health Research Network financially supports the Uveal Melanoma Biobank and the Eye Tissue Bank.

## Compliance with ethical standards

**Conflict of interest** The authors disclose no conflicts of interest.

## References

- Landreville S, Agapova OA, Harbour JW (2008) Emerging insights into the molecular pathogenesis of uveal melanoma. *Future Oncol* 4(5):629–636. <https://doi.org/10.2217/14796694.4.5.629>
- Singh AD, Bergman L, Seregard S (2005) Uveal melanoma: epidemiologic aspects. *Ophthalmol Clin North Am* 18(1):75–84. <https://doi.org/10.1016/j.ohc.2004.07.002>
- Kujala E, Makitie T, Kivela T (2003) Very long-term prognosis of patients with malignant uveal melanoma. *Invest Ophthalmol Vis Sci* 44(11):4651–4659
- Diener-West M, Reynolds SM, Agugliaro DJ, Caldwell R, Cumming K, Earle JD, Hawkins BS, Hayman JA, Jaiyesimi I, Jampol LM, Kirkwood JM, Koh WJ, Robertson DM, Shaw JM, Straatsma BR, Thoma J (2005) Development of metastatic disease after enrollment in the COMS trials for treatment of choroidal melanoma: collaborative ocular melanoma study group report No. 26. *Arch Ophthalmol* 123(12):1639–1643. <https://doi.org/10.1001/archophth.123.12.1639>
- Augsburger JJ, Gamel JW (1990) Clinical prognostic factors in patients with posterior uveal malignant melanoma. *Cancer* 66(7):1596–1600
- Albert DM, Diener-West M, Robinson NL, Grossniklaus HE, Green WR, Vine AK, Willis J, Frueh B, Kurtz RM, Elner S, Johnson MW (1998) Histopathologic characteristics of uveal melanomas in eyes enucleated from the Collaborative Ocular Melanoma Study. COMS report no. 6. *Am J Ophthalmol* 125(6):745–766
- Sisley K, Rennie IG, Parsons MA, Jacques R, Hammond DW, Bell SM, Potter AM, Rees RC (1997) Abnormalities of chromosomes 3 and 8 in posterior uveal melanoma correlate with prognosis. *Genes Chromosom Cancer* 19(1):22–28
- Harbour JW, Onken MD, Roberson ED, Duan S, Cao L, Worley LA, Council ML, Matattal KA, Helms C, Bowcock AM (2010) Frequent mutation of BAP1 in metastasizing uveal melanomas. *Science* 330(6009):1410–1413. <https://doi.org/10.1126/science.1194472>
- Harbour JW, Chen R (2013) The Decisiondx-UM gene expression profile test provides risk stratification and individualized patient care in uveal melanoma. *PLoS Curr*. <https://doi.org/10.1371/currents.eogt.af8ba80fc776c8f1ce8f5dc485d4a618>
- Onken MD, Worley LA, Tuscan MD, Harbour JW (2010) An accurate, clinically feasible multi-gene expression assay for predicting metastasis in uveal melanoma. *J Mol Diagn* 12(4):461–468. <https://doi.org/10.2353/jmoldx.2010.090220>
- Choi DS, Ward SJ, Messaddeq N, Launay JM, Maroteaux L (1997) 5-HT2B receptor-mediated serotonin morphogenetic functions in mouse cranial neural crest and myocardial cells. *Development* 124(9):1745–1755
- Raymond JR, Mukhin YV, Gelasco A, Turner J, Collinsworth G, Gettys TW, Grewal JS, Garnovskaya MN (2001) Multiplicity of mechanisms of serotonin receptor signal transduction. *Pharmacol Ther* 92(2–3):179–212
- Launay JM, Birraux G, Bondoux D, Callebert J, Choi DS, Loric S, Maroteaux L (1996) Ras involvement in signal transduction by the serotonin 5-HT2B receptor. *J Biol Chem* 271(6):3141–3147
- Nebigil CG, Launay JM, Hickel P, Tournois C, Maroteaux L (2000) 5-hydroxytryptamine 2B receptor regulates cell-cycle progression: cross-talk with tyrosine kinase pathways. *Proc Natl Acad Sci USA* 97(6):2591–2596. <https://doi.org/10.1073/pnas.050282397>
- Onken MD, Worley LA, Long MD, Duan S, Council ML, Bowcock AM, Harbour JW (2008) Oncogenic mutations in GNAQ occur early in uveal melanoma. *Invest Ophthalmol Vis Sci* 49(12):5230–5234. <https://doi.org/10.1167/iovs.08-2145>
- Van Raamsdonk CD, Bezrookove V, Green G, Bauer J, Gaugler L, O'Brien JM, Simpson EM, Barsh GS, Bastian BC (2009) Frequent somatic mutations of GNAQ in uveal melanoma and blue naevi. *Nature* 457(7229):599–602. <https://doi.org/10.1038/nature07586>
- Van Raamsdonk CD, Griewank KG, Crosby MB, Garrido MC, Vemula S, Wiesner T, Obenaus AC, Wackernagel W, Green G, Bouvier N, Sozen MM, Baimukanova G, Roy R, Heguy A, Dalgalev I, Khanin R, Busam K, Speicher MR, O'Brien J, Bastian BC (2010) Mutations in GNA11 in uveal melanoma. *N Engl J Med* 363(23):2191–2199. <https://doi.org/10.1056/NEJMoa1000584>
- De Lucchini S, Ori M, Nardini M, Marracci S, Nardi I (2003) Expression of 5-HT2B and 5-HT2C receptor genes is associated with proliferative regions of Xenopus developing brain and eye. *Brain Res Mol Brain Res* 115(2):196–201
- Dizeyi N, Bjartell A, Hedlund P, Tasken KA, Gadaleanu V, Abrahamsson PA (2005) Expression of serotonin receptors 2B and 4 in human prostate cancer tissue and effects of their antagonists on prostate cancer cell lines. *Eur Urol* 47(6):895–900. <https://doi.org/10.1016/j.eururo.2005.02.006>
- Kopparapu PK, Tinzl M, Anagnostaki L, Persson JL, Dizeyi N (2013) Expression and localization of serotonin receptors in human breast cancer. *Anticancer Res* 33(2):363–370
- Svejda B, Kidd M, Giovino F, Eltawil K, Gustafsson BI, Pfragner R, Modlin IM (2010) The 5-HT(2B) receptor plays a key regulatory role in both neuroendocrine tumor cell proliferation and the modulation of the fibroblast component of the neoplastic microenvironment. *Cancer* 116(12):2902–2912. <https://doi.org/10.1002/cncr.25049>

22. Soll C, Jang JH, Riener MO, Moritz W, Wild PJ, Graf R, Clavien PA (2010) Serotonin promotes tumor growth in human hepatocellular cancer. *Hepatology* 51(4):1244–1254. <https://doi.org/10.1002/hep.23441>
23. Jiang SH, Li J, Dong FY, Yang JY, Liu DJ, Yang XM, Wang YH, Yang MW, Fu XL, Zhang XX, Li Q, Pang XF, Huo YM, Li J, Zhang JF, Lee HY, Lee SJ, Qin WX, Gu JR, Sun YW, Zhang ZG (2017) Increased serotonin signaling contributes to the warburg effect in pancreatic tumor cells under metabolic stress and promotes growth of pancreatic tumors in mice. *Gastroenterology* 153(1):277–291. <https://doi.org/10.1053/j.gastro.2017.03.008>
24. Henriksen R, Dizayi N, Abrahamsson PA (2012) Expression of serotonin receptors 5-HT1A, 5-HT1B, 5-HT2B and 5-HT4 in ovary and in ovarian tumours. *Anticancer Res* 32(4):1361–1366
25. Landreville S, Vigneault F, Bergeron MA, Leclerc S, Gaudreault M, Morcos M, Mouriaux F, Salesse C, Guerin SL (2011) Suppression of alpha5 gene expression is closely related to the tumorigenic properties of uveal melanoma cell lines. *Pigm Cell Melanoma Res* 24(4):643–655. <https://doi.org/10.1111/j.1755-148X.2011.00869.x>
26. Mouriaux F, Zaniolo K, Bergeron MA, Weidmann C, De La Fouchardiere A, Fournier F, Droit A, Morcos MW, Landreville S, Guerin SL (2016) Effects of long-term serial passaging on the characteristics and properties of cell lines derived from uveal melanoma primary tumors. *Invest Ophthalmol Vis Sci* 57(13):5288–5301. <https://doi.org/10.1167/iovs.16-19317>
27. Mouriaux F, Sanschagrin F, Diorio C, Landreville S, Comoz F, Petit E, Bernaudin M, Rousseau AP, Bergeron D, Morcos M (2014) Increased HIF-1alpha expression correlates with cell proliferation and vascular markers CD31 and VEGF-A in uveal melanoma. *Invest Ophthalmol Vis Sci* 55(3):1277–1283. <https://doi.org/10.1167/iovs.13-13345>
28. Bergeron MA, Champagne S, Gaudreault M, Deschambeault A, Landreville S (2012) Repression of genes involved in melanocyte differentiation in uveal melanoma. *Mol Vis* 18:1813–1822
29. Hu DN, McCormick SA, Ritch R, Pelton-Henrion K (1993) Studies of human uveal melanocytes in vitro: isolation, purification and cultivation of human uveal melanocytes. *Invest Ophthalmol Vis Sci* 34(7):2210–2219
30. de la Fouchardiere A, Cabaret O, Savin L, Combemale P, Schwartz H, Penet C, Bonadona V, Soufir N, Bressac-de Paillerets B (2015) Germline BAP1 mutations predispose also to multiple basal cell carcinomas. *Clin Genet* 88(3):273–277. <https://doi.org/10.1111/cge.12472>
31. Landreville S, Agapova OA, Kneass ZT, Salesse C, Harbour JW (2011) ABCB1 identifies a subpopulation of uveal melanoma cells with high metastatic propensity. *Pigm Cell Melanoma Res* 24(3):430–437. <https://doi.org/10.1111/j.1755-148X.2011.00841.x>
32. Gilda JE, Gomes AV (2015) Western blotting using in-gel protein labeling as a normalization control: stain-free technology. *Methods Mol Biol* 1295:381–391. [https://doi.org/10.1007/978-1-4939-2550-6\\_27](https://doi.org/10.1007/978-1-4939-2550-6_27)
33. Posch A, Kohn J, Oh K, Hammond M, Liu N (2013) V3 stain-free workflow for a practical, convenient, and reliable total protein loading control in western blotting. *J Vis Exp* 82:50948. <https://doi.org/10.3791/50948>
34. Cory AH, Owen TC, Barltrop JA, Cory JG (1991) Use of an aqueous soluble tetrazolium/formazan assay for cell growth assays in culture. *Cancer Commun* 3(7):207–212
35. Porvasnik SL, Germain S, Embury J, Gannon KS, Jacques V, Murray J, Byrne BJ, Shacham S, Al-Mousily F (2010) PRX-08066, a novel 5-hydroxytryptamine receptor 2B antagonist, reduces monocrotaline-induced pulmonary arterial hypertension and right ventricular hypertrophy in rats. *J Pharmacol Exp Ther* 334(2):364–372. <https://doi.org/10.1124/jpet.109.165001>
36. West JD, Carrier EJ, Bloodworth NC, Schroer AK, Chen P, Ryzhova LM, Gladson S, Shay S, Hutcheson JD, Merryman WD (2016) Serotonin 2B receptor antagonism prevents heritable pulmonary arterial hypertension. *PLoS ONE* 11(2):e0148657. <https://doi.org/10.1371/journal.pone.0148657>
37. Launay JM, Herve P, Peoc'h K, Tournois C, Callebert J, Nebigil CG, Etienne N, Drouet L, Humbert M, Simonneau G, Maroteaux L (2002) Function of the serotonin 5-hydroxytryptamine 2B receptor in pulmonary hypertension. *Nat Med* 8(10):1129–1135. <https://doi.org/10.1038/nm764>
38. Mucke HA (2001) Mt-500 (Pozen). *Curr Opin Invest Drugs* 2(3):419–421
39. Panconesi A, Sicuteri R (1997) Headache induced by serotonergic agonists—a key to the interpretation of migraine pathogenesis? *Cephalalgia* 17(1):3–14
40. Borman RA, Tilford NS, Harmer DW, Day N, Ellis ES, Sheldrick RL, Carey J, Coleman RA, Baxter GS (2002) 5-HT(2B) receptors play a key role in mediating the excitatory effects of 5-HT in human colon in vitro. *Br J Pharmacol* 135(5):1144–1151. <https://doi.org/10.1038/sj.bjp.0704571>
41. Spiller R (2008) Serotonergic agents and the irritable bowel syndrome: what goes wrong? *Curr Opin Pharmacol* 8(6):709–714. <https://doi.org/10.1016/j.coph.2008.07.003>
42. Masters JR (2000) Human cancer cell lines: fact and fantasy. *Nat Rev Mol Cell Biol* 1(3):233–236. <https://doi.org/10.1038/35043102>
43. Kielhorn E, Provost E, Olsen D, D'Aquila TG, Smith BL, Camp RL, Rimm DL (2003) Tissue microarray-based analysis shows phospho-beta-catenin expression in malignant melanoma is associated with poor outcome. *Int J Cancer* 103(5):652–656. <https://doi.org/10.1002/ijc.10893>
44. Zuidervaart W, Pavey S, van Nieuwpoort FA, Packer L, Out C, Maat W, Jager MJ, Gruis NA, Hayward NK (2007) Expression of Wnt5a and its downstream effector beta-catenin in uveal melanoma. *Melanoma Res* 17(6):380–386. <https://doi.org/10.1097/CMR.0b013e3282f1d302>
45. Yoo JH, Shi DS, Grossmann AH, Sorensen LK, Tong Z, Mleynek TM, Rogers A, Zhu W, Richards JR, Winter JM, Zhu J, Dunn C, Bajji A, Shenderovich M, Mueller AL, Woodman SE, Harbour JW, Thomas KR, Odelberg SJ, Ostanin K, Li DY (2016) ARF6 Is an actionable node that orchestrates oncogenic GNAQ signaling in uveal melanoma. *Cancer Cell* 29(6):889–904. <https://doi.org/10.1016/j.ccell.2016.04.015>
46. Sinnberg T, Menzel M, Ewerth D, Sauer B, Schwarz M, Schaller M, Garbe C, Schitteck B (2011) Beta-Catenin signaling increases during melanoma progression and promotes tumor cell survival and chemoresistance. *PLoS ONE* 6(8):e23429. <https://doi.org/10.1371/journal.pone.0023429>
47. Levy DE, Gilliland DG (2000) Divergent roles of STAT1 and STAT5 in malignancy as revealed by gene disruptions in mice. *Oncogene* 19(21):2505–2510. <https://doi.org/10.1038/sj.onc.1203480>
48. Wellbrock C, Weisser C, Hassel JC, Fischer P, Becker J, Vetter CS, Behrmann I, Kortylewski M, Heinrich PC, Schartl M (2005) STAT5 contributes to interferon resistance of melanoma cells. *Curr Biol* 15(18):1629–1639. <https://doi.org/10.1016/j.cub.2005.08.036>
49. Mirmohammadsadegh A, Hassan M, Bardenheuer W, Marini A, Gustrau A, Nambiar S, Tannapfel A, Bojar H, Ruzicka T, Hengge UR (2006) STAT5 phosphorylation in malignant melanoma is important for survival and is mediated through SRC and JAK1 kinases. *J Invest Dermatol* 126(10):2272–2280. <https://doi.org/10.1038/sj.jid.5700385>
50. Williams KE, Bundred NJ, Landberg G, Clarke RB, Farnie G (2015) Focal adhesion kinase and Wnt signaling regulate human ductal carcinoma in situ stem cell activity and response to

- radiotherapy. *Stem Cells* 33(2):327–341. <https://doi.org/10.1002/stem.1843>
51. Fan H, Guan JL (2011) Compensatory function of Pyk2 protein in the promotion of focal adhesion kinase (FAK)-null mammary cancer stem cell tumorigenicity and metastatic activity. *J Biol Chem* 286(21):18573–18582. <https://doi.org/10.1074/jbc.M110.200717>
  52. Roelle S, Grosse R, Buech T, Chubanov V, Gudermann T (2008) Essential role of Pyk2 and Src kinase activation in neuropeptide-induced proliferation of small cell lung cancer cells. *Oncogene* 27(12):1737–1748. <https://doi.org/10.1038/sj.onc.1210819>
  53. Fu B, Meng W, Zhao H, Zhang B, Tang H, Zou Y, Yao J, Li H, Zhang T (2016) GRAM domain-containing protein 1A (GRAMD1A) promotes the expansion of hepatocellular carcinoma stem cell and hepatocellular carcinoma growth through STAT5. *Sci Rep* 6:31963. <https://doi.org/10.1038/srep31963>
  54. Selitrennik M, Lev S (2015) PYK2 integrates growth factor and cytokine receptors signaling and potentiates breast cancer invasion via a positive feedback loop. *Oncotarget* 6(26):22214–22226. <https://doi.org/10.18632/oncotarget.4257>
  55. Sun CK, Man K, Ng KT, Ho JW, Lim ZX, Cheng Q, Lo CM, Poon RT, Fan ST (2008) Proline-rich tyrosine kinase 2 (Pyk2) promotes proliferation and invasiveness of hepatocellular carcinoma cells through c-Src/ERK activation. *Carcinogenesis* 29(11):2096–2105. <https://doi.org/10.1093/carcin/bgn203>
  56. Zhang S, Qiu X, Gu Y, Wang E (2008) Up-regulation of proline-rich tyrosine kinase 2 in non-small cell lung cancer. *Lung Cancer* 62(3):295–301. <https://doi.org/10.1016/j.lungcan.2008.05.008>
  57. Fatima S, Shi X, Lin Z, Chen GQ, Pan XH, Wu JC, Ho JW, Lee NP, Gao H, Zhang G, Lu A, Bian ZX (2016) 5-Hydroxytryptamine promotes hepatocellular carcinoma proliferation by influencing beta-catenin. *Mol Oncol* 10(2):195–212. <https://doi.org/10.1016/j.molonc.2015.09.008>
  58. Sui H, Xu H, Ji Q, Liu X, Zhou L, Song H, Zhou X, Xu Y, Chen Z, Cai J, Ji G, Li Q (2015) 5-hydroxytryptamine receptor (5-HT<sub>1DR</sub>) promotes colorectal cancer metastasis by regulating Axin1/beta-catenin/MMP-7 signaling pathway. *Oncotarget* 6(28):25975–25987. <https://doi.org/10.18632/oncotarget.4543>
  59. Homsy J, Cubitt C, Daud A (2007) The Src signaling pathway: a potential target in melanoma and other malignancies. *Expert Opin Ther Targets* 11(1):91–100. <https://doi.org/10.1517/1472822.11.1.91>
  60. Qi J, Wang J, Romanyuk O, Siu CH (2006) Involvement of Src family kinases in N-cadherin phosphorylation and beta-catenin dissociation during transendothelial migration of melanoma cells. *Mol Biol Cell* 17(3):1261–1272. <https://doi.org/10.1091/mbc.E05-10-0927>
  61. Dikic I, Tokiwa G, Lev S, Courtneidge SA, Schlessinger J (1996) A role for Pyk2 and Src in linking G-protein-coupled receptors with MAP kinase activation. *Nature* 383(6600):547–550. <https://doi.org/10.1038/383547a0>
  62. Zhao M, Finlay D, Zharkikh I, Vuori K (2016) Novel role of Src in priming Pyk2 phosphorylation. *PLoS ONE* 11(2):e0149231. <https://doi.org/10.1371/journal.pone.0149231>
  63. Gao C, Chen G, Kuan SF, Zhang DH, Schlaepfer DD, Hu J (2015) FAK/PYK2 promotes the Wnt/beta-catenin pathway and intestinal tumorigenesis by phosphorylating GSK3beta. *Elife*. <https://doi.org/10.7554/eLife.10072>
  64. van Buul JD, Anthony EC, Fernandez-Borja M, Burridge K, Hordijk PL (2005) Proline-rich tyrosine kinase 2 (Pyk2) mediates vascular endothelial-cadherin-based cell-cell adhesion by regulating beta-catenin tyrosine phosphorylation. *J Biol Chem* 280(22):21129–21136. <https://doi.org/10.1074/jbc.M500898200>
  65. Lee TK, Man K, Poon RT, Lo CM, Yuen AP, Ng IO, Ng KT, Leonard W, Fan ST (2006) Signal transducers and activators of transcription 5b activation enhances hepatocellular carcinoma aggressiveness through induction of epithelial-mesenchymal transition. *Cancer Res* 66(20):9948–9956. <https://doi.org/10.1158/0008-5472.CAN-06-1092>
  66. Yang Q, Yan C, Yin C, Gong Z (2017) Serotonin activated hepatic stellate cells contribute to sex disparity in hepatocellular carcinoma. *Cell Mol Gastroenterol Hepatol* 3(3):484–499. <https://doi.org/10.1016/j.jcmgh.2017.01.002>
  67. Ebrahimkhani MR, Oakley F, Murphy LB, Mann J, Moles A, Perugorria MJ, Ellis E, Lakey AF, Burt AD, Douglass A, Wright MC, White SA, Jaffre F, Maroteaux L, Mann DA (2011) Stimulating healthy tissue regeneration by targeting the 5-HT<sub>2B</sub> receptor in chronic liver disease. *Nat Med* 17(12):1668–1673. <https://doi.org/10.1038/nm.2490>
  68. Kang N, Gores GJ, Shah VH (2011) Hepatic stellate cells: partners in crime for liver metastases? *Hepatology* 54(2):707–713. <https://doi.org/10.1002/hep.24384>